



Research papers

Estimation of global reservoir evaporation losses

Wei Tian^{a,b}, Xiaomang Liu^{a,*}, Kaiwen Wang^{a,b}, Peng Bai^a, Changming Liu^a, Xijin Liang^c^a Key Laboratory of Water Cycle & Related Land Surface Process, Institute of Geographic Sciences and Natural Resources Research, Chinese Academy of Sciences, 100101 Beijing, China^b University of Chinese Academy of Sciences, Beijing, China^c Haihe River Water Conservancy Commission, Ministry of Water Resources of the People's Republic of China, Tianjin, China

ARTICLE INFO

This manuscript was handled by Marco Borga, Editor-in-Chief, with the assistance of Lixin Wang, Associate Editor.

Keywords:

Reservoir evaporation
Water resources management
Global scale
Middle-income countries

ABSTRACT

Estimating global reservoir evaporation losses is essential for reservoir regulation, operation, and associated water resources management. Estimating globe-scale reservoir evaporation losses remains a gap due to limited accessibility of global long-term continuous reservoir geographic information. Two new datasets, the Global Reservoir Surface Area Dataset and the Global Reservoir and Dam Database, try to address inaccessibility and provide an opportunity to bridge the gap. Here, we used the two datasets to estimate the monthly reservoir evaporation volume of global 7242 large reservoirs from 1985 to 2016. Around 339.8 km³ of water is estimated to evaporate from these large reservoirs annually during 1985–2016, and the loss amount is near ~73% of the municipal water withdrawal in 2010. From 1985 to 2016, the global reservoir evaporation volume increases significantly at a rate of ~2.0 km³/a, and 80% of the increment is contributed by middle-income countries. A surge in reservoir construction in middle-income countries after 1985 triggers the increment. The results can benefit the regulation and operation of reservoirs and realize their role in global water conservation and management.

1. Introduction

As an ancient water storage infrastructure, the reservoir has been built for ~4000 years, and currently, there are still millions of reservoirs with an area of over 100 m² in operation over the world (Assouline et al., 2011; Lehner et al., 2011; Zarfl et al., 2015). Reservoirs serve a pivotal role in agricultural and municipal water storage and deliveries (Tharme, 2003; Prigent et al., 2012), yet the role is impacted by reservoir evaporation loss (Shiklomanov, 2000; Martínez-Granados et al., 2011; Zhan et al., 2019; Jansen and Teuling, 2020). It is estimated that annual mean reservoir evaporation loss in the United States is more than 90% of its annual public water supply (Zhao and Gao, 2019a), the annual loss in China is ~80% of water delivery volume for the Middle Route of China's Water Transfer Project (Tian et al., 2021), and annual loss in Africa is over 80% of the water storage capacity of Cahora Bassa, Africa's fourth-largest hydropower reservoir (Sanchez et al., 2021). Thus, estimating reservoir evaporation loss is important in water conservation and management.

Estimating reservoir evaporation, indeed, requires specific geographic information and hydro-climatic data (Lowe et al., 2009; Reca et al., 2015), while due to involving national and regional security,

it is restricted to access the geographic information of reservoirs. Constrained by data accessibility, existing estimates of reservoir evaporation are carried out on limited temporal scales and spatial scales (Helfer et al., 2012; Rodrigues et al., 2020). The spatial scale of the reservoir evaporation estimation is mainly conducted on national and regional scales as exemplified by estimations in the United States (Zhao and Gao, 2019a; Zhang et al., 2017), China (Tian et al., 2021), Africa (Sanchez et al., 2021), as well as some watersheds in Spain (Alvarez et al., 2008) and Australia (Craig et al., 2005). The temporal scale of the reservoir evaporation estimation is generally focused on a certain year (e.g., Craig et al., 2005; Rodrigues et al., 2020; Sanchez et al., 2021) or averages in a period of time (e.g., Alvarez et al., 2008; Helfer et al., 2012). Consequently, limited accessibility of global long-term continuous reservoir geographic information leads to estimating global dynamic reservoir evaporation remains to be explored.

Recently, international data sharing and the development of remote sensing observations make it possible to obtain global long-term continuous geographic data of reservoirs. The international Global Water System Project promotes the collation of existing geographic data of global reservoirs and shares the collation as the Global Reservoir and Dam Database (GRaND), which includes static geographic data of

* Corresponding author.

E-mail address: liuxm@igsnr.ac.cn (X. Liu).<https://doi.org/10.1016/j.jhydrol.2022.127524>

Received 22 November 2021; Received in revised form 4 January 2022; Accepted 21 January 2022

Available online 29 January 2022

0022-1694/© 2022 Elsevier B.V. All rights reserved.

reservoirs, such as location, shape, and multi-year average surface area, etc. (Lehner et al., 2011). This dataset has been keeping updated, from version 1.1 in 2011 to 1.3 in 2019, and is widely applied in reservoir research on a global scale (e.g., Donchyts et al., 2016; Grill et al., 2019; Frederikse et al., 2020). The static geographic data of global reservoirs in GRaND, together with the lately development of remote sensing observations, gave birth to a global long-term continuous geographic data of reservoirs, i.e., the Global Reservoir Surface Area Dataset (GRSAD, Zhao and Gao, 2018). The recent emerge of GRaND and GRSAD, accordingly, provide an opportunity to estimate global long-term continuous reservoir evaporation.

Based on GRaND and GRSAD, here, we estimate the global long-term continuous reservoir evaporation using the Penman equation. Such a globe-scale estimation can benefit the regulation and operation of reservoirs and thus realize their role in global water conservation and management. In this paper, we first introduced the data and methodology in Section 2, and then estimated and investigated changes of reservoir evaporation on a global scale in Section 3. Finally, the discussion and conclusions of this paper are given in Sections 4 and 5, respectively.

2. Data used and methods

2.1. Data used

The surface area and basic information of the global reservoirs were provided by the Global Reservoir Surface Area Dataset (GRSAD) and the Global Reservoir and Dam Database (GRaND), respectively. For the surface area, GRSAD provided the monthly data from 1985 to 2016. For basic information, GRaND provided information on water storage capacity, dam location, and reservoir depth, etc. Based on the two databases, the data of 7242 reservoirs were collected. The number of these reservoirs increased from 6028 to 7242 during 1985–2016, and these reservoirs are distributed in 137 countries over the world (Fig. 1).

The evaporation calculation needs four meteorological variables, namely, vapor pressure deficit (VPD), wind speed (u), surface shortwave radiation (SSR), and air temperature (T_a). Monthly data of the four variables were provided by three datasets viz. (1) TerraClimate (Abatzoglou et al., 2018); (2) ERA5 (Hersbach et al., 2020); (3) Princeton Global Forcings (PGF, Sheffield et al., 2006). Spatial resolutions of the three datasets are $1/24^\circ \times 1/24^\circ$, $0.25^\circ \times 0.25^\circ$, and $0.25^\circ \times 0.25^\circ$, respectively. Here, the temporal resolutions of the three datasets are all monthly, and time ranges are all from 1985 to 2016.

The reservoir is a vital infrastructure, and its construction, especially for large reservoirs, requires huge economic investment and can also

bring significant economic profit. Thus, the number of reservoirs built in a country is closely related to the country's economic level. The level could be measured by the income of the country. Based on the classification of countries by income of the World Bank (Fantom and Serajuddin, 2016), the 137 countries in this study were divided into four groups, namely high-income countries, upper-middle-income countries, lower-middle-income countries, and low-income countries. Here, the four groups include 48, 42, 29, and 18 countries, respectively.

2.2. Methodology of estimation in the reservoir evaporation volume

The reservoir evaporation volume is determined by the evaporation rate and surface area of the reservoir (Lowe et al., 2009; Reca et al., 2015). For a single reservoir, the monthly evaporation volume can be calculated as follows:

$$E_{volume} = A \times E \times D \times 1000 \quad (1)$$

where A [km^2] is the monthly surface area for a single reservoir, which was obtained from the GRSAD in this study (Zhao and Gao, 2018, 2019b); D [d] is the number of days in the calculated month; E [mm/d] is the monthly evaporation rate for a single reservoir, and E_{volume} [m^3] is the evaporation volume for a single reservoir in the calculated month.

The methods to estimate the reservoir evaporation rate of open water can be classified into energy- and process-based models. The energy-based model used the surface available energy and the Bowen ratio to estimate evaporation rate, such as the Conceptual Atmospheric Boundary Layer Model (Liu and Yang, 2021), etc. The process-based model includes the Penman equation (Penman, 1948), variations of the Penman equation (Monteith, 1965; Priestley & Taylor, 1972), and the pan coefficient method (Rotstayn et al., 2006; Lim et al., 2012; Lim et al., 2013), etc. The pan coefficient method uses the product of the recommended pan coefficient and measured or estimated pan evaporation rate as the reservoir evaporation rate (Yang and Yang, 2012; Lim et al., 2016; Wang et al., 2019a,b), and this method cannot consider the impact of water body heat storage on open water evaporation rate (Kisi, 2006; Friedrich et al., 2018; Zhao and Gao, 2019a). The impact can be considered in the Penman equation and its variations, and these methods can be more accurately estimated the open water evaporation rate. Moreover, the Penman equation has been validated in many studies to estimate the evaporation rate of open water, and this equation was used in this study to calculate the reservoir evaporation rate (McMahon et al., 2013). The reservoir evaporation rate is estimated by using the sum of the radiative (E_R) and the aerodynamic (E_A) components:

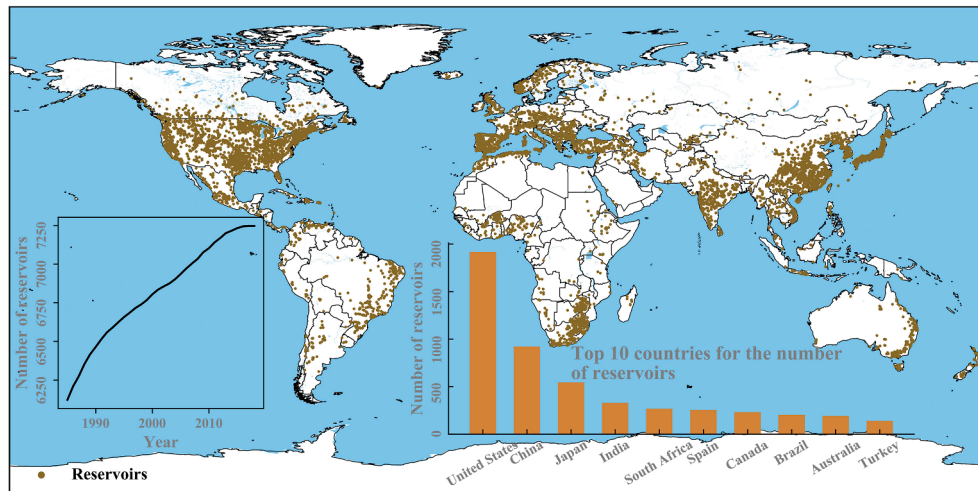


Fig. 1. Locations of the 7242 reservoirs over the world.

$$E = \underbrace{\frac{s(R_n - \Delta U)}{\lambda_v(s + \gamma)}}_{E_R} + \underbrace{\frac{\gamma f(u)(e_s - e_a)}{\lambda_v(s + \gamma)}}_{E_A} \quad (2)$$

where R_n [MJ/(m²d)] is the monthly net radiation for a single reservoir; s [kPa/°C] is the slope of the saturation vapor pressure curve; γ [kPa/°C] is the psychrometric constant; λ_v [MJ/kg] is the latent heat of vaporization; e_a [kPa] is the air vapor pressure at T_a ; ΔU [MJ/(m²d)] is the change of water body heat storage for a single reservoir; e_s [kPa] is the saturated vapor pressure at T_a , and $f(u)$ [MJ/(m²dkPa)] is the wind function.

The wind function $f(u)$ is the key factor of the calculation of E_A . When calculating reservoir evaporation, the meteorological data should use observation from the water surface. Due to lack of observation, most studies have employed land-based data as a substitute (Winter et al., 1995; dos Reis and Dias, 1998; McJannet et al., 2012), which may bring a biased estimation of reservoir evaporation (Weisman and Brutsaert, 1973). To reduce estimation biases, the area-dependent wind function based on the aerodynamic approach was developed, which can directly use land-based meteorological data to calculate (McJannet et al., 2012). Here, this wind function was adopted to calculate E_A .

$$f(u) = \lambda_v(2.33 + 1.65u_2)L_f^{-0.1} \quad (3)$$

where u_2 [m/s] is the wind speed measured at 2 m; and L_f [m] is the fetch length for a single reservoir. The fetch length was estimated by dividing the reservoir surface area by the reservoir width. The width is defined as the distance between two reservoir tangents parallel to the wind direction (McJannet et al., 2012; Zhao and Gao, 2019a).

A key factor of the calculation of E_R is the change of water body heat storage ΔU . Here, the equilibrium temperature method was adopted to estimate the ΔU (Edinger et al., 1968; McMahon et al., 2013):

$$T_e = \frac{(k\varepsilon_w + f(u)(s + \gamma))T_a + (1 - \alpha)K\downarrow - b(\varepsilon_w - \varepsilon_a) - f(u)(e_s - e_a)}{k\varepsilon_w + f(u)(s + \gamma)} \quad (4)$$

$$T_w = T_e + (T_{wo} - T_e)e^{-\Delta t/\tau} \quad (5)$$

$$T_{wb} = \frac{0.00066 * 100T_a + \frac{4098e_a}{(T_d + 237.3)^2} T_d}{0.00066 * 100 + \frac{4098e_a}{(T_d + 237.3)^2}} \quad (6)$$

$$T_d = \frac{116.9 + 237.3 \ln(e_a)}{16.78 + \ln(e_a)} \quad (7)$$

$$\tau = \frac{\rho_w c_w \bar{h}}{4\sigma(T_{wb} + 273.15)^3 + f(u)(s_{wb} + \gamma)} \quad (8)$$

$$\Delta U = \rho_w c_w \bar{h} \frac{T_w - T_{wo}}{\Delta t} \quad (9)$$

where T_{wb} [°C] and T_e [°C] are wet-bulk temperatures and the equilibrium temperature of water body, respectively; T_w [°C] and T_{wo} [°C] are actual water column temperatures at the current time and previous time, respectively, and the initial value of T_{wo} is obtained by spin-up; T_d [°C] is the dew point temperature; α is water surface albedo, and the value is 0.1; k and b are constants, and the values are 0.46 MJ/(m²d°C) and 23.38 MJ/(m²d), respectively; s_{wb} [kPa/°C] is the slope of the saturation vapor pressure curve at T_{wb} ; ε_a is the emissivity of air with cloudiness factor (Satterlund, 1979); ε_w is the emissivity of water, here, it was set 0.97; $K\downarrow$ [MJ/(m²d)] is the downward surface shortwave radiation; τ [d] is the lag time; ρ_w [kg/m³] is the density of water; \bar{h} [m] is the average reservoir depth, and limited by the availability of data, the value is constant from the Rand; c_w [MJ/(kg°C)] is the specific heat of the water.

The detailed methodology flow chart and related equations can be referenced in Zhao and Gao (2019a). The methodology has been validated in the estimations of reservoir evaporation volume in China and the United States (Zhao and Gao, 2019a; Tian et al., 2021). The

estimation using a single dataset as forcing data could bring uncertainty. To reduce the uncertainty, the ensemble estimation of the reservoir evaporation volume calculated using ERA5, TerraClimate, and PGF, as the robust estimations in this study. In addition, all the trends below were and tested by the two-tailed Mann-Kendall test of significance (Mann, 1945; Kendall, 1975) and evaluated by the nonparametric Sen's slope.

3. Result

3.1. Significant increase in global reservoir evaporation losses

Here, the annual global reservoir evaporation volume is the sum of the evaporation volume of all reservoirs that year. During 1985–2016, the annual mean global reservoir evaporation volume was 339.8 km³ (Fig. 2(a)), which is about 73% of the global municipal water withdrawal in 2010 (~464 km³, FAO, 2016). Table 1 shows the ranking of the ten countries with the largest annual average reservoir evaporation volume from 1985 to 2016. The two high-income countries, namely Canada and the United States, had the largest annual average reservoir evaporation volume, with values of 58.6 km³ and 43.1 km³ respectively, accounting for about 30% of the annual average global reservoir evaporation volume. The rest eight countries are all middle-income countries (including 4 upper-middle-income countries and 4 lower-middle-income countries), whose total annual mean reservoir evaporation volume accounts for about 40% of the annual mean global reservoir evaporation volume.

From 1985 to 2016, the global reservoir evaporation volume shows a significant ($p < 0.05$) increasing trend at a rate of 2.0 km³/a, and increased from 292.1 km³ to 364.0 km³ (Fig. 2(b)). Among the 137 countries, the total reservoir evaporation volume in 29 countries shown decreasing trends, with 14 countries passing the significance test ($p < 0.05$) (Fig. 2(b)). These countries with decreasing trends are prominently clustered in Central Asia and Central Africa—most notably in Iraq, which had a significant ($p < 0.05$) decreasing trend at a rate of -9.4×10^7 m³/a. For the rest 108 countries, the total reservoir evaporation volume all shown increasing trends, with 81 countries passing the significance test ($p < 0.05$). Among these countries, Brazil's increasing trend was most notably, with a significant ($p < 0.05$) trend of 47.8×10^7 m³/a. Table 2 shows the ranking of the ten countries with the largest trend of reservoir evaporation volume from 1985 to 2016. Eight of these ten countries are middle-income countries (including 6 upper-middle-income countries and 2 lower-middle-income countries).

3.2. Increase in reservoir surface area is the dominant driver of the increase in global reservoir evaporation volume

The change in global reservoir evaporation volume was determined by changes in average evaporation rate and total surface area. The change in total surface area was greatly affected by the number of the reservoir. From 1985 to 2016, 1264 new reservoirs, 17% of total reservoirs (1264/7242), were constructed globally, thus these new reservoirs could affect the change in global reservoir evaporation volume. Here, the changes of the global reservoir evaporation volume were analyzed for two types of reservoirs, i.e., reservoirs built before 1985 and after 1985. The total evaporation volume for the two types of reservoirs both significantly ($p < 0.05$) increased from 1985 to 2016, with rates of 0.32 km³/a and 1.70 km³/a, respectively (Fig. 3(a)). 85% (=1.70/2.01) of trend in global evaporation volume were contributed by reservoirs built after 1985. Therefore, the total global evaporation volume of 7242 reservoirs was mainly driven by the total evaporation volume of 1214 reservoirs built after 1985.

The reservoir evaporation volume was determined by the evaporation rate and surface area of the reservoir. During 1985–2016, the total surface area of the 1214 reservoirs built after 1985 significantly ($p < 0.05$) increased at a rate of 1307.2 km²/a, while the mean evaporation

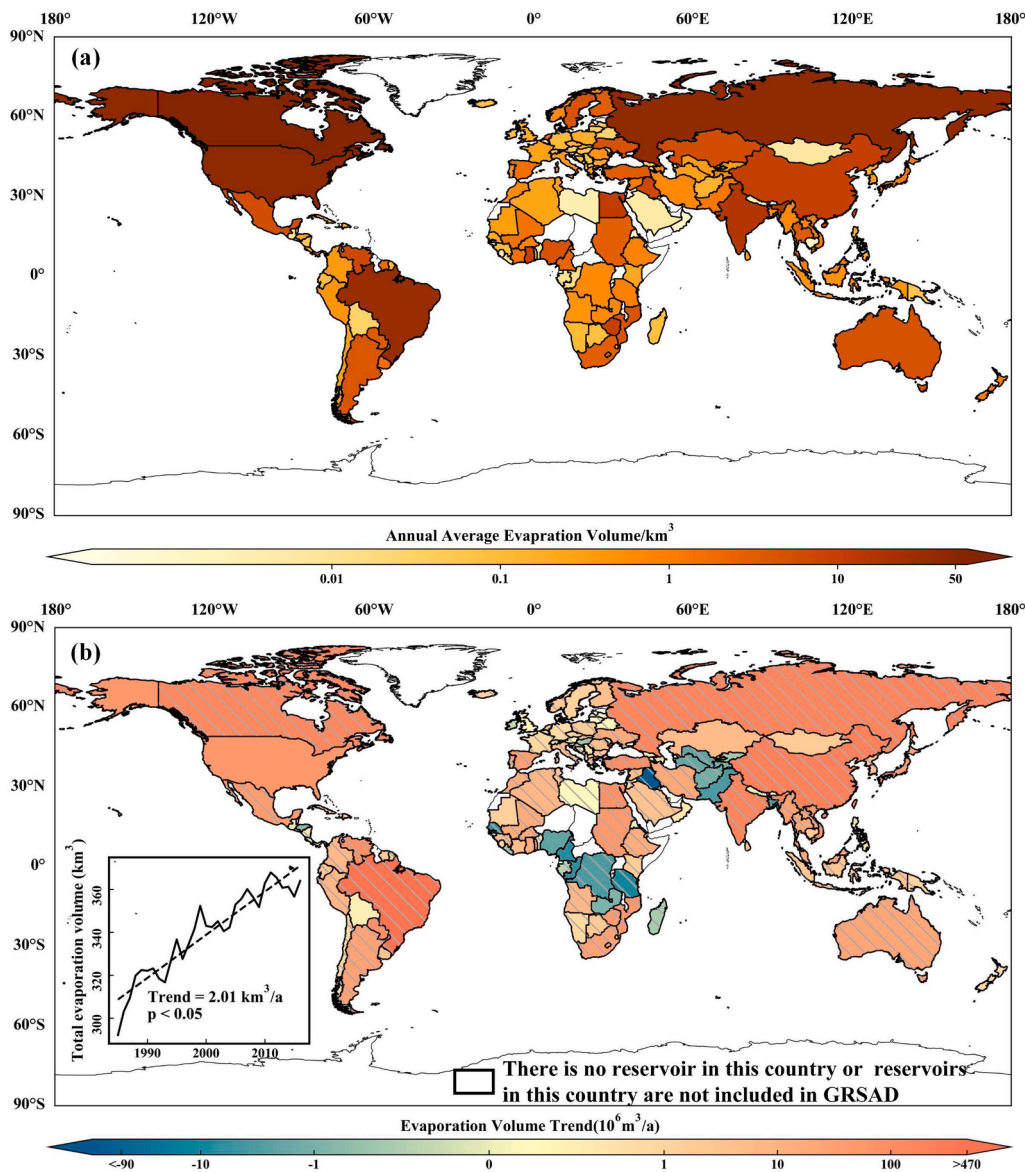


Fig. 2. Map of annual average (a) and trend (b) of reservoir evaporation volume on the national scale from 1985 to 2016. The slash indicates that the trend passes the significance test ($p < 0.05$).

Table 1

Ranking of the 10 countries with the largest annual average reservoir evaporation volume from 1985 to 2016.

Rank	Country	Evaporation Volume (km^3)	Income Level
1	Canada	58.6	High
2	United States	43.1	High
3	Russia	39.0	Upper-middle
4	Brazil	32.7	Upper-middle
5	India	15.2	Lower-middle
6	Egypt	11.4	Lower-middle
7	China	10.7	Upper-middle
8	Ghana	10.0	Lower-middle
9	Zimbabwe	9.8	Lower-middle
10	Venezuela	7.1	Upper-middle

rate insignificantly ($p = 0.12$) increased at a rate of 0.001 mm/d/a (Fig. 3). The main reason for the significant increase in total evaporation of 1214 reservoirs built after 1985 was the significant increase in total surface area. Therefore, the total global evaporation volume of 7242 reservoirs was mainly driven by the total surface area of the 1214

Table 2

Ranking of the 10 countries with the largest trend of reservoir evaporation volume during 1985–2016.

Rank	Country	Trend ($10^7 \text{ m}^3/\text{a}$)	Level
1	Brazil	47.8*	Upper-middle
2	China	20.2*	Upper-middle
3	India	15.6*	Lower-middle
4	Russia	15.3*	Upper-middle
5	Canada	12.1*	High
6	Turkey	8.8*	Upper-middle
7	Venezuela	7.0*	Upper-middle
8	Paraguay	7.0*	Upper-middle
9	Egypt	6.9*	Lower-middle
10	United States	5.0	High

*indicates that the trend passes the significance test ($p < 0.05$).

reservoirs built after 1985.

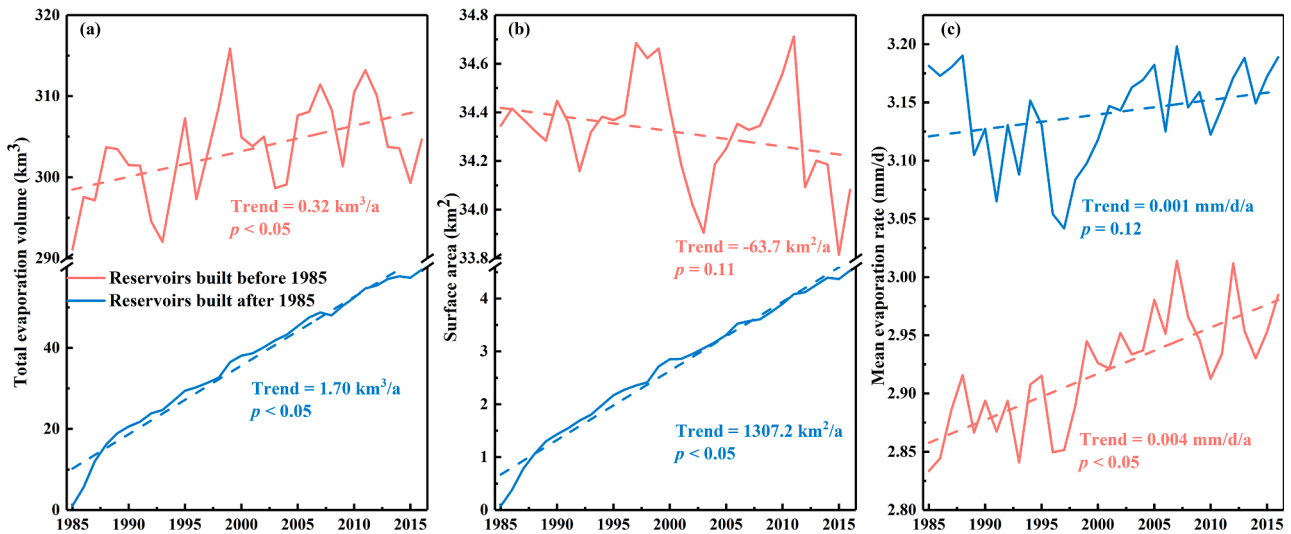


Fig. 3. Total reservoir evaporation volume (a), total reservoir surface areas (b), and mean reservoir evaporation rate (c) during 1985–2016 for reservoirs built before and after 1985.

3.3. The increase in surface area of reservoirs in the middle-income countries dominates the increase in global surface area

From 1985 to 2016, the total surface area of reservoirs all showed significant ($p < 0.05$) increasing trends for the four group countries, namely high-income countries, upper-middle-income countries, lower-middle-income countries, and low-income countries, with values of 228.2, 743.4, 226.5, and 45.4 km^2/a , respectively. The increase in total surface area of reservoirs of middle-income countries, including upper-middle-income and lower-middle-income countries accounts for 78% ($= (743.4 + 226.5) / (228.2 + 743.4 + 226.5 + 45.4)$) of the increase in total global surface area (Fig. 4(a)).

Focus on the reservoirs built before 1985, the total surface area of the upper-middle-income countries during 1985–2016 significantly ($p < 0.05$) decreased at a rate of $-95.9 \text{ km}^2/\text{a}$, while the total surface area of the lower-middle-income countries was nonsignificant ($p = 0.40$) increasing at a rate of $17.8 \text{ km}^2/\text{a}$ (Fig. 4(b)). Above all, the total surface area of reservoirs built before 1985 in middle-income countries decreased at a rate of $-78.1 \text{ km}^2/\text{a}$ ($= -95.9 + 17.8$). Focus on the reservoirs after 1985, the total surface area for the two group middle-

income countries, namely upper-middle-income countries, lower-middle-income countries, both significantly ($p < 0.05$) increased from 1985 to 2016, with rates of $839.4 \text{ km}^2/\text{a}$ and $208.8 \text{ km}^2/\text{a}$, respectively (Fig. 4(c)). Above all, the total surface area of reservoirs built after 1985 in middle-income countries decreased at a rate of $1058.2 \text{ km}^2/\text{a}$ ($= 839.4 + 208.8$). 109% ($= 1058.2 / (743.4 + 226.5)$) of trend in total surface area in middle-income countries was contributed by reservoirs built after 1985. Therefore, the total surface area of middle-income countries was mainly driven by the reservoirs built after 1985.

Above all, the change of the total evaporation volume in middle-income countries had a significant impact on the change of the global evaporation volume. From 1985 to 2016, the increase in total evaporation volume in middle-income countries accounts for 80% ($(1.15 + 0.46) / (0.31 + 1.15 + 0.46 + 0.09)$) of the increase in global evaporation volume (Fig. 5(a)). Further, 90% ($(1.09 + 0.36) / (1.15 + 0.46)$) of the trend in the total evaporation volume in middle-income countries was contributed by reservoirs built after 1985 (Fig. 5(b, c)). Therefore, the global evaporation volume was mainly driven by the reservoirs built after 1985 in middle-income countries.

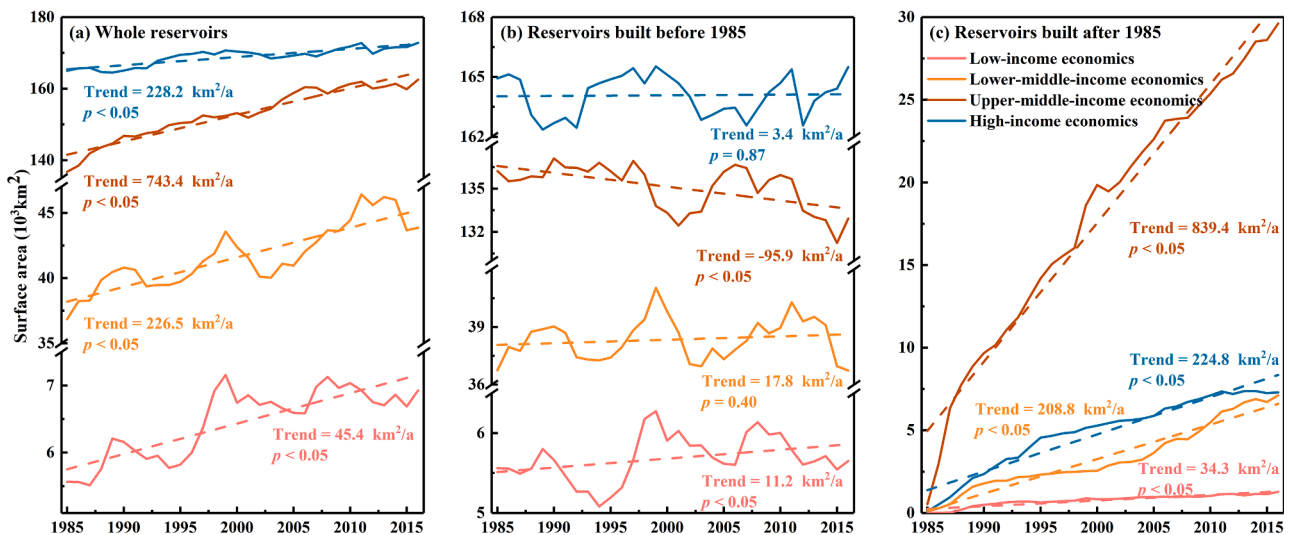


Fig. 4. Total reservoir surface area for the four groups countries, namely high, upper-middle, lower-middle, and low, during 1985–2016 for whole reservoirs (a), reservoirs built before 1985 (b), and reservoirs built after 1985 (c).

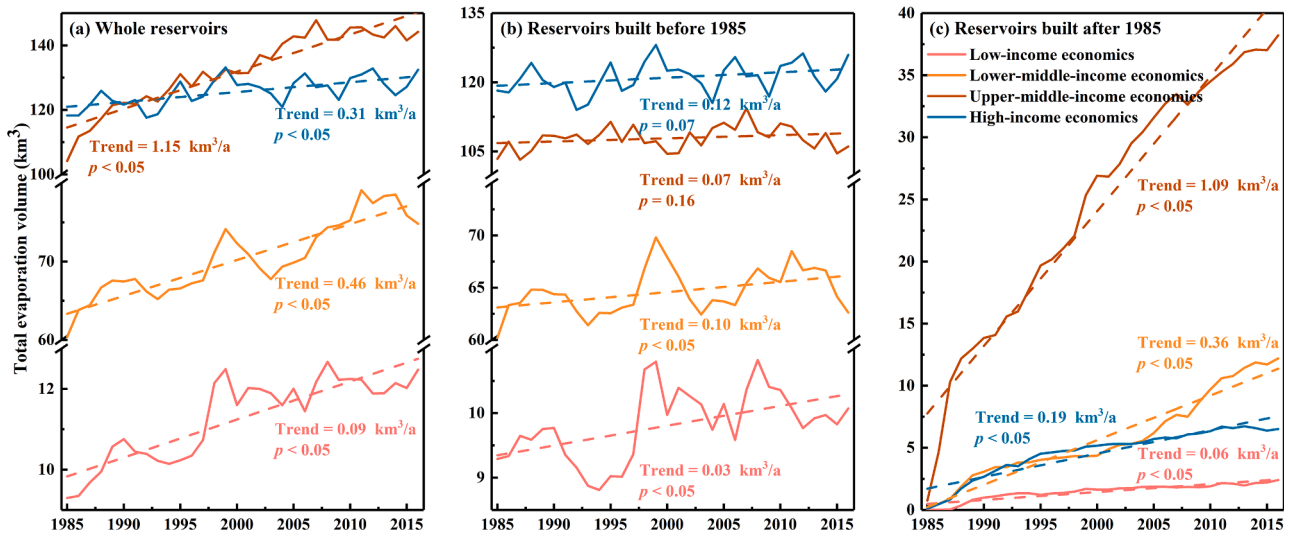


Fig. 5. Total reservoir evaporation volumes for the four groups countries, namely high, upper-middle, lower-middle, and low, during 1985–2016 for whole reservoirs (a), reservoirs built before 1985 (b), and reservoirs built after 1985 (c).

4. Discussion

4.1. Uncertainties of estimating the reservoir evaporation losses

There are some uncertainties in this study. First, there are some uncertainties in the meteorological data used to estimate the reservoir evaporation rate. The three meteorological datasets, namely the TerraClimate, ERA5, and PGF, were used to calculate the evaporation rate. The three datasets are inconsistent on some meteorological variables. For instance, the average surface shortwave radiation over the 7242 reservoirs for the three datasets, namely TerraClimate, ERA5, and PGF, were 176.7 W/m^2 , 183.4 W/m^2 , and 186.8 W/m^2 , respectively. The differences of meteorological variables in the three datasets resulted in different reservoir evaporation estimations. The annual average global reservoir evaporation volumes calculated were 319.1 km^3 , 336.5 km^3 , and 364.8 km^3 during 1985–2016 for the three datasets, respectively (Fig. 6). The trends of annual global evaporation volumes were $1.92 \text{ km}^3/\text{a}$, $2.05 \text{ km}^3/\text{a}$, and $2.07 \text{ km}^3/\text{a}$ for the three datasets, respectively. Thus, to obtain a robust estimation, the ensemble average of the three estimations was shown in this study. Second, there are some uncertainties in the method used to estimate the reservoir evaporation rate. Generally, the methods of estimating evaporation rate included energy-

and process-based models. Here, the process-based model, the Penman equation incorporated with the heat storage, was used, which has been validated in the estimation of reservoir evaporation (Zhao and Gao, 2019a; Tian et al., 2021). The energy-based model also shows the accurate estimation in water evaporation rate, such as the conceptual atmospheric boundary layer model (ABL, Liu and Yang, 2021). The estimation of this model in China's Lake Taihu shown good consistency with the measurements of the eddy covariance (EC). As a comparison, the method in this study was used to estimate the water evaporation rate in Lake Taihu (Fig. S1). The estimation also shown good consistent with the measurements of the EC ($R^2 = 0.90$, $RMSE = 0.47 \text{ mm}$). Thus, the uncertainty of only using the Penman model to estimate the evaporation rate could be limited. Third, the ice sublimation cannot be calculated by using the Penman method for reservoir evaporation rate estimation. Once the T_a drops below 0°C , the reservoir water surface would freeze. This situation usually occurs in the winter in high latitude areas ($\geq 50^\circ \text{N}$ and $\geq 40^\circ \text{S}$). In this study, there are 457 reservoirs located in the high latitude area, accounting for 6.3% of the total 7242 reservoirs. The reservoir evaporation estimation of these reservoirs would bring some uncertainties to global reservoir evaporation volume.

4.2. Comparisons with previous studies

Here, the reservoir evaporation losses and their change for global and countries were estimated during 1984–2016. For country-scale estimations, Zhao and Gao (2019a) and Tian et al. (2021) calculated the reservoir evaporation losses for the world's largest developed and developing countries, namely the United States and China, respectively. They indicated that the average annual evaporation losses of 721 and 916 large reservoirs (storage capacity greater than 0.1 km^3) were 33.7 km^3 and 10.5 km^3 for the two countries, respectively, and the trend were $6.6 \times 10^7 \text{ m}^3/\text{a}$ ($p = 0.02$) and $19.6 \times 10^7 \text{ m}^3/\text{a}$ ($p < 0.01$), respectively. The losses estimation and their trend for the same number of reservoirs in this study are in good agreement with previous studies (losses: 33.7 km^3 vs 34.4 km^3 , 10.5 km^3 vs 10.2 km^3 ; trend: $6.6 \times 10^7 \text{ m}^3/\text{a}$ vs $5.3 \times 10^7 \text{ m}^3/\text{a}$, $19.6 \times 10^7 \text{ m}^3/\text{a}$ vs $20.2 \times 10^7 \text{ m}^3/\text{a}$).

The significant increase in total reservoir evaporation losses is mainly driven by the increase in total surface area, especially in middle-income countries. Zhan et al. (2019) reported the consistent view that one of the main reasons for the increase in global water surface evaporation is the increase in the total reservoir area, especially Brazil and India, etc. Mao et al. (2016) illustrated that the change in total reservoir area had a significant impact on evapotranspiration trends over China.

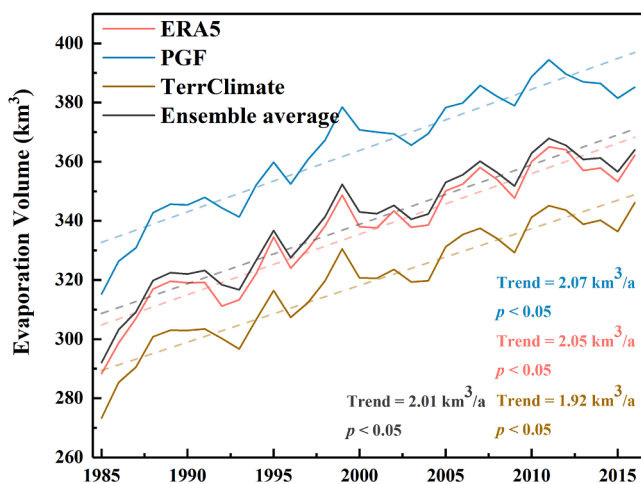


Fig. 6. The global evaporation volumes during 1985–2016 calculated using ERA5, PGF, TerraClimate and ensemble average.

In addition, due to the diversion of water from the Amu Darya and the Syr Darya for agricultural irrigation in Central Asia (Micklin, 1988; Micklin, 2014; Wang et al., 2018), the total water surface area was severely reduced (Micklin, 2014; Shi et al., 2014). The reduction could lead to a significant decrease in reservoir evaporation losses in Central Asia (Fig. 2).

4.3. Implications

The estimation of the global reservoir evaporation losses can benefit the regional or global water resources management. First, the estimation can be used to calculate the available water resources for the reservoir (Tanny et al., 2008; Lowe et al., 2009; Khadem et al., 2018; Zhang et al., 2019). For a single reservoir, the available water resources is estimated based on the water balance equation, and the equation needs various variables, namely, inflow, outflow, precipitation, and reservoir evaporation. Based on the current observation methods, accurate observations can be obtained in the inflow, outflow, precipitation of the reservoir. Thus, accurate estimation of reservoir evaporation can be used to calculate the available water resources of the reservoir (Sivapragasam et al., 2009; Campos, 2010; Lei and Yang, 2010; Althoff et al., 2019; Hu and Lei, 2021). Second, reservoir evaporation estimation can be used to calculate water-saving efficiency. Reservoir evaporation losses cannot be ignored for local water resources management, especially for water resources management in semi-arid and arid regions (Morton, 1979; Ali et al., 2008; Mady et al., 2020). To reduce reservoir evaporation losses, the various shelters are covered on the reservoir water surface. The water-saving efficiency of the shelter is an important index for selecting shelters. The efficiency is calculated by dividing observed or calculated reservoir evaporation under the shelter by reservoir open water evaporation estimation (Yao et al., 2010; Aminzadeh et al., 2018; Lehmann et al., 2019). Third, reservoir evaporation estimation can be used to estimate the evaporation reduction potential of floating photovoltaic (FPV). FPV system is a new power generation system that places the photovoltaic system on the reservoir surface (Sahu et al., 2016; Ranjbaran et al., 2019). The system can not only generate power, but also reduce evaporation from the reservoir (Ferrer-Gisbert et al., 2013; Santafé et al., 2014; Redón-Santafé et al., 2014). Based on the reservoir evaporation estimation and FPV coverage of the reservoir, the evaporation reduction potential of the FPV can be calculated (Spencer et al., 2019; Scavo et al., 2021; Nagananthini and Nagavinothini, 2021; Sanchez et al., 2021).

5. Conclusions

Here, the monthly reservoir evaporations during 1985–2016 for the 7242 large reservoirs over the world were estimated. The annual average global reservoir evaporation volume of all reservoirs during 1985–2016 was 339.8 km³, which is about 73% of the global municipal water withdrawal in 2010 (~464 km³). The two high-income countries, namely Canada and the United States, have the largest reservoir evaporation volume among all countries, with values of 58.6 km³ and 43.1 km³ respectively. The total global reservoir evaporation volume increased significantly ($p < 0.05$) during 1985–2016 from 292.1 km³ to 364.0 km³ at a rate of 2.0 km³/a. The significant increment in global reservoir evaporation volume was mainly driven by the total surface area of all reservoirs. The increase in surface area of the reservoirs built after 1985 in middle-income countries dominated the increase in global reservoir surface area. The results can support the regulation and operation of reservoirs and realize their role in global water conservation and management.

Declaration of Competing Interest

The authors declare that they have no known competing financial interests or personal relationships that could have appeared to influence

the work reported in this paper.

Acknowledgments

This work was supported by the National Natural Science Foundation of China (No. 41922050) and the Youth Innovation Promotion Association, Chinese Academy of Sciences (2018067). This research benefited from the TerraClimate dataset (https://developers.google.com/earth-engine/datasets/catalog/IDAHO_EPSCOR_TERRACLIMATE), ERA5 (<https://www.ecmwf.int/en/forecasts/datasets/reanalysis-datasets/era5>), Princeton Global Forcings (<https://hydrology.princeton.edu/data.pgf.php>), the Global Reservoir Surface Area Dataset (<https://dataverse.tdl.org/dataset.xhtml?persistentId=doi:10.18738/T8/DF80WG>), and the Global Reservoir and Dam Database (<http://global-damwatch.org/grand/>). All of the authors acknowledge Editor Marco Borga, Associate Editor Lixin Wang and two anonymous reviewers for their invaluable comments and constructive suggestions for this research.

Appendix A. Supplementary data

Supplementary data to this article can be found online at <https://doi.org/10.1016/j.jhydrol.2022.127524>.

References

- Assouline, S., Narkis, K., Or, D., 2011. Evaporation suppression from water reservoirs: Efficiency considerations of partial covers. *Water Resour. Res.* 47 (7) <https://doi.org/10.1029/2010WR009889>.
- Abatzoglou, J.T., Dobrowski, S.Z., Parks, S.A., Hegewisch, K.C., 2018. TerraClimate, a high-resolution global dataset of monthly climate and climatic water balance from 1958–2015. *Sci. Data* 5, 170191. <https://doi.org/10.1038/sdata.2017.191>.
- Ali, S., Ghosh, N.C., Singh, R., 2008. Evaluating best evaporation estimate model for water surface evaporation in semi-arid region. *India. Hydrological Processes: An International Journal* 22 (8), 1093–1106.
- Althoff, D., Rodrigues, L.N., da Silva, D.D., Bazame, H.C., 2019. Improving methods for estimating small reservoir evaporation in the Brazilian Savanna. *Agric. Water Manag.* 216, 105–112.
- Alvarez, V.M., González-Real, M.M., Baille, A., Valero, J.M., Elvira, B.G., 2008. Regional assessment of evaporation from agricultural irrigation reservoirs in a semiarid climate. *Agric. Water Manag.* 95 (9), 1056–1066. <https://doi.org/10.1016/j.agwat.2008.04.003>.
- Aminzadeh, M., Lehmann, P., Or, D., 2018. Evaporation suppression and energy balance of water reservoirs covered with self-assembling floating elements. *Hydrol. Earth Syst. Sci.* 22 (7), 4015–4032.
- Campos, J.N.B., 2010. Modeling the yield–evaporation–spill in the reservoir storage process: The regulation triangle diagram. *Water Resour. Manage.* 24 (13), 3487–3511.
- Craig, I., Green, A., Scobie, M., Schmidt, E., 2005. Controlling evaporation loss from water storages, No. 1000580/1. NCEA Publication, (Queensland, Australia).
- Donchyts, G., Baart, F., Winsemius, H., Gorelick, N., Kwadijk, J., van de Giesen, N., 2016. Earth's surface water change over the past 30 years. *Nat. Clim. Change* 6 (9), 810–813.
- dos Reis, R.J., Dias, N.L., 1998. Multi-season lake evaporation: energy-budget estimates and CRLE model assessment with limited meteorological observations. *J. Hydrol.* 208 (3–4), 135–147.
- Edinger, J.E., Duttweiler, D.W., Geyer, J.C., 1968. The response of water temperatures to meteorological conditions. *Water Resour. Res.* 4 (5), 1137–1143.
- FAO. 2016. AQUASTAT database. <http://www.fao.org/nr/water/aquastat/data/query/index.html?lang=en>.
- Fantom, N., Serajuddin, U., 2016. The World Bank's classification of countries by income. The World Bank.
- Ferrer-Gisbert, C., Ferrán-Gozálvez, J.J., Redón-Santafé, M., Ferrer-Gisbert, P., Sánchez-Romero, F.J., Torregrosa-Soler, J.B., 2013. A new photovoltaic floating cover system for water reservoirs. *Renewable Energy* 60, 63–70.
- Friedrich, K., Grossman, R. L., Huntington, J., Blanken, P. D., Lenters, J., Holman, K. D., ... & Kowalski, T. (2018). Reservoir evaporation in the Western United States: current science, challenges, and future needs. *Bulletin of the American Meteorological Society*, 99(1), 167–187. <https://doi.org/10.1175/BAMS-D-15-00224.1>.
- Frederikse, T., Landerer, F., Caron, L., Adhikari, S., Parkes, D., Humphrey, V.W., Wu, Y. H., 2020. The causes of sea-level rise since 1900. *Nature* 584 (7821), 393–397.
- Grill, G., Lehner, B., Thieme, M., Geenen, B., Tickner, D., Antonelli, F., Zarfl, C., 2019. Mapping the world's free-flowing rivers. *Nature* 569 (7755), 215–221.
- Helfer, F., Lemckert, C., Zhang, H., 2012. Impacts of climate change on temperature and evaporation from a large reservoir in Australia. *J. Hydrol.* 475, 365–378. <https://doi.org/10.1016/j.jhydrol.2012.10.008>.

- Hersbach, H., Bell, B., Berrisford, P., Hirahara, S., Horányi, A., Muñoz-Sabater, J., Nicolas, J., Peubey, C., Radu, R., Schepers, D., Simmons, A., Soci, C., Abdalla, S., Abellan, X., Balsamo, G., Bechtold, P., Biavati, G., Bidlot, J., Bonavita, M., Chiara, G., Dahlgren, P., Dee, D., Diamantakis, M., Dragani, R., Flemming, J., Forbes, R., Fuentes, M., Geer, A., Haimberger, L., Healy, S., Hogan, R.J., Hólm, E., Janisková, M., Keeley, S., Lalouaux, P., Lopez, P., Lupu, C., Radnoti, G., Rosnay, P., Rozum, I., Vamborg, F., Villaume, S., Thépaut, J.-N., 2020. The ERA5 global reanalysis. *Q. J. R. Meteorol. Soc.* 146 (730), 1999–2049. <https://doi.org/10.1002/qj.146.73010.1002/qj.3803>.
- Hu, X., Lei, H., 2021. Evapotranspiration partitioning and its interannual variability over a winter wheat-summer maize rotation system in the North China Plain. *Agric. For. Meteorol.* 310, 108635. <https://doi.org/10.1016/j.agrformet.2021.108635>.
- Jansen, F.A., Teuling, A.J., 2020. Evaporation from a large lowland reservoir—(dis) agreement between evaporation models from hourly to decadal timescales. *Hydrol. Earth Syst. Sci.* 24 (3), 1055–1072.
- Kendall, K., 1975. Thin-film peeling—the elastic term. *J. Phys. D Appl. Phys.* 8 (13), 1449–1452.
- Khadem, M., Rougé, C., Harou, J.J., Hansen, K.M., Medellin-Azuara, J., Lund, J.R., 2018. Estimating the economic value of interannual reservoir storage in water resource systems. *Water Resour. Res.* 54 (11), 8890–8908.
- Kiş, Ö., 2006. Daily pan evaporation modelling using a neuro-fuzzy computing technique. *J. Hydrol.* 329 (3–4), 636–646. <https://doi.org/10.1016/j.jhydrol.2006.03.015>.
- Lehmann, P., Aminzadeh, M., Or, D., 2019. Evaporation suppression from water bodies using floating covers: laboratory studies of cover type, wind, and radiation effects. *Water Resour. Res.* 55 (6), 4839–4853.
- Lehner, B., Liermann, C.R., Revenga, C., Vörösmarty, C., Fekete, B., Crouzet, P., Döll, P., Endejan, M., Frenken, K., Magome, J., Nilsson, C., Robertson, J.C., Rödel, R., Sindorf, N., Wissler, D., 2011. High-resolution mapping of the world's reservoirs and dams for sustainable river-flow management. *Front. Ecol. Environ.* 9 (9), 494–502. <https://doi.org/10.1890/100125>.
- Lei, H., Yang, D., 2010. Interannual and seasonal variability in evapotranspiration and energy partitioning over an irrigated cropland in the North China Plain. *Agric. For. Meteorol.* 150 (4), 581–589.
- Lim, W.H., Roderick, M.L., Hobbins, M.T., Wong, S.C., Groeneveld, P.J., Sun, F., Farquhar, G.D., 2012. The aerodynamics of pan evaporation. *Agric. For. Meteorol.* 152, 31–43.
- Lim, W.H., Roderick, M.L., Hobbins, M.T., Wong, S.C., Farquhar, G.D., 2013. The energy balance of a US Class A evaporation pan. *Agric. For. Meteorol.* 182–183, 314–331.
- Lim, W.H., Roderick, M.L., Farquhar, G.D., 2016. A mathematical model of pan evaporation under steady state conditions. *J. Hydrol.* 540, 641–658. <https://doi.org/10.1016/j.jhydrol.2016.06.048>.
- Liu, Z., & Yang, H. (2021). Estimation of water surface energy partitioning with a conceptual atmospheric boundary layer model. *Geophysical Research Letters*, 48(9), e2021GL092643.
- Lowe, L.D., Webb, J.A., Nathan, R.J., Etschells, T., Malano, H.M., 2009. Evaporation from water supply reservoirs: An assessment of uncertainty. *J. Hydrol.* 376 (1–2), 261–274. <https://doi.org/10.1016/j.jhydrol.2009.07.037>.
- Mady, B., Lehmann, P., Gorelick, S.M., Or, D., 2020. Distribution of small seasonal reservoirs in semi-arid regions and associated evaporative losses. *Environmental Research Communications* 2 (6), 061002. <https://doi.org/10.1088/2515-7620/ab92af>.
- Mann, H.B., 1945. Nonparametric tests against trend. *Econometrica: Journal of the econometric society* 13 (3), 245. <https://doi.org/10.2307/1907187>.
- Mao, Y., Wang, K., Liu, X., Liu, C., 2016. Water storage in reservoirs built from 1997 to 2014 significantly altered the calculated evapotranspiration trends over China. *Journal of Geophysical Research: Atmospheres* 121 (17), 10–097.
- Martínez-Granados, D., Maestre-Valero, J.F., Calatrava, J., Martínez-Alvarez, V., 2011. The economic impact of water evaporation losses from water reservoirs in the Segura basin. SE Spain. *Water Resources Management* 25 (13), 3153–3175.
- McJannet, D.L., Webster, I.T., Cook, F.J., 2012. An area-dependent wind function for estimating open water evaporation using land-based meteorological data. *Environ. Modell. Software* 31, 76–83. <https://doi.org/10.1016/j.envsoft.2011.11.017>.
- McMahon, T.A., Peel, M.C., Lowe, L., Srikanthan, R., McVicar, T.R., 2013. Estimating actual, potential, reference crop and pan evaporation using standard meteorological data: a pragmatic synthesis. *Hydrol. Earth Syst. Sci.* 17 (4), 1331–1363. <https://doi.org/10.5194/hess-17-1331-2013>.
- Micklin, P.P., 1988. Desiccation of the Aral Sea: a water management disaster in the Soviet Union. *Science* 241 (4870), 1170–1176.
- Micklin, P., 2014. In: *The Aral Sea*. Springer Berlin Heidelberg, Berlin, Heidelberg, pp. 361–380. https://doi.org/10.1007/978-3-642-02356-9_15.
- Monteith, J.L., 1965. Evaporation and environment. In *Symposia of the society for experimental biology* Vol. 19, 205–234.
- Morton, F.I., 1979. Climatological estimates of lake evaporation. *Water Resour. Res.* 15 (1), 64–76.
- Nagananthini, R., Nagavinothini, R., 2021. Investigation on floating photovoltaic covering system in rural Indian reservoir to minimize evaporation loss. *Int. J. Sustain. Energ.* 40 (8), 781–805.
- Penman, H.L., 1948. Natural evaporation from open water, bare soil and grass. *Proc. R. Soc. Lond. A* 193 (1032), 120–145. <https://doi.org/10.1098/rspa.1948.0037>.
- Priestley, C.H.B., Taylor, R.J., 1972. On the assessment of surface heat flux and evaporation using large-scale parameters. *Mon. Weather Rev.* 100 (2), 81–92. [https://doi.org/10.1175/1520-0493\(1972\)100<0081:OTAOSH>2.3.CO;2](https://doi.org/10.1175/1520-0493(1972)100<0081:OTAOSH>2.3.CO;2).
- Prigent, C., Papa, F., Aires, F., Jimenez, C., Rossow, W.B., Matthews, E., 2012. Changes in land surface water dynamics since the 1990s and relation to population pressure. *Geophys. Res. Lett.* 39 (8), n/a–n/a. <https://doi.org/10.1029/2012GL051276>.
- Ranjbaran, P., Yousefi, H., Gharehpetian, G.B., Astaraei, F.R., 2019. A review on floating photovoltaic (FPV) power generation units. *Renew. Sustain. Energy Rev.* 110, 332–347.
- Reca, J., García-Manzano, A., Martínez, J., 2015. Optimal pumping scheduling model considering reservoir evaporation. *Agric. Water Manag.* 148, 250–257. <https://doi.org/10.1016/j.agwat.2014.10.008>.
- Redón-Santafé, M.R., Ferrer Gisbert, P.S., Sánchez Romero, F.J., Torregrosa Soler, J.B., Ferrán Gozálviz, J.J., Ferrer Gisbert, C.M., 2014. Implementation of a photovoltaic floating cover for irrigation reservoirs. *J. Cleaner Prod.* 66, 568–570.
- Rodrigues, C.M., Moreira, M., Guimarães, R.C., Potes, M., 2020. Reservoir evaporation in a Mediterranean climate: comparing direct methods in Alqueva Reservoir. *Portugal. Hydrology and Earth System Sciences* 24 (12), 5973–5984. <https://doi.org/10.5194/hess-24-5973-2020>.
- Rotstayn, L.D., Roderick, M.L., Farquhar, G.D., 2006. A simple pan-evaporation model for analysis of climate simulations: Evaluation over Australia. *Geophys. Res. Lett.* 33 (17) <https://doi.org/10.1029/2006GL027114>.
- Sahu, A., Yadav, N., Sudhakar, K., 2016. Floating photovoltaic power plant: A review. *Renew. Sustain. Energy Rev.* 66, 815–824.
- Sanchez, R.G., Kougijs, I., Moner-Girona, M., Fahl, F., Jäger-Waldau, A., 2021. Assessment of floating solar photovoltaics potential in existing hydropower reservoirs in Africa. *Renewable Energy* 169, 687–699.
- Santafé, M.R., Torregrosa Soler, J.B., Sánchez Romero, F.J., Ferrer Gisbert, P.S., Ferrán Gozálviz, J.J., Ferrer Gisbert, C.M., 2014. Theoretical and experimental analysis of a floating photovoltaic cover for water irrigation reservoirs. *Energy* 67, 246–255.
- Satterlund, D.R., 1979. An improved equation for estimating long-wave radiation from the atmosphere. *Water Resour. Res.* 15 (6), 1649–1650.
- Scavo, F.B., Tina, G.M., Gagliano, A., Nizetić, S., 2021. An assessment study of evaporation rate models on a water basin with floating photovoltaic plants. *Int. J. Energy Res.* 45 (1), 167–188.
- Sheffield, J., Goteti, G., Wood, E.F., 2006. Development of a 50-year high-resolution global dataset of meteorological forcings for land surface modeling. *J. Clim.* 19 (13), 3088–3111. <https://doi.org/10.1175/JCLI3790.1>.
- Shi, W., Wang, M., Guo, W., 2014. Long-term hydrological changes of the Aral Sea observed by satellites. *J. Geophys. Res. Oceans* 119 (6), 3313–3326.
- Shiklomanov, I.A., 2000. Appraisal and assessment of world water resources. *Water Int.* 25 (1), 11–32.
- Sivapragasam, C., Vasudevan, G., Maran, J., Bose, C., Kaza, S., Ganesh, N., 2009. Modeling evaporation-seepage losses for reservoir water balance in semi-arid regions. *Water Resour. Manage.* 23 (5), 853–867.
- Spencer, R.S., Macknick, J., Aznar, A., Warren, A., Reese, M.O., 2019. Floating photovoltaic systems: assessing the technical potential of photovoltaic systems on man-made water bodies in the continental United States. *Environ. Sci. Technol.* 53 (3), 1680–1689.
- Tanny, J., Cohen, S., Assouline, S., Lange, F., Grava, A., Berger, D., Teltch, B., Parlange, M.B., 2008. Evaporation from a small water reservoir: Direct measurements and estimates. *J. Hydrol.* 351 (1–2), 218–229.
- Tharme, R.E., 2003. A global perspective on environmental flow assessment: emerging trends in the development and application of environmental flow methodologies for rivers. *River Res. Appl.* 19 (5–6), 397–441.
- Tian, W., Liu, X., Wang, K., Bai, P., Liu, C., 2021. Estimation of reservoir evaporation losses for China. *J. Hydrol.* 596, 126142. <https://doi.org/10.1016/j.jhydrol.2021.126142>.
- Wang, K., Liu, X., Liu, C., Yang, X., Bai, P., Li, Y., Pan, Z., 2019a. The unignorable impacts of pan wall on pan evaporation dynamics. *Agric. For. Meteorol.* 274, 42–50.
- Wang, K., Liu, X., Tian, W., Li, Y., Liang, K., Liu, C., Li, Y., Yang, X., 2019b. Pan coefficient sensitivity to environment variables across China. *J. Hydrol.* 572, 582–591. <https://doi.org/10.1016/j.jhydrol.2019.03.039>.
- Wang, J., Song, C., Reager, J.T., Yao, F., Famiglietti, J.S., Sheng, Y., MacDonald, G.M., Brun, F., Schmied, H.M., Marston, R.A., Wada, Y., 2018. Recent global decline in endorheic basin water storages. *Nat. Geosci.* 11 (12), 926–932.
- Weisman, R.N., Brutsaert, W., 1973. Evaporation and cooling of a lake under unstable atmospheric conditions. *Water Resour. Res.* 9 (5), 1242–1257.
- Winter, T.C., Rosenberry, D.O., Sturrock, A.M., 1995. Evaluation of 11 equations for determining evaporation for a small lake in the north central United States. *Water Resour. Res.* 31 (4), 983–993.
- Yao, X., Zhang, H., Lemckert, C., Brook, A., Schouten, P., 2010. Evaporation reduction by suspended and floating covers: overview, modelling and efficiency. In: *Urban water security research alliance technical report*, p. 28.
- Yang, H., Yang, D., 2012. Climatic factors influencing changing pan evaporation across China from 1961 to 2001. *J. Hydrol.* 414–415, 184–193.
- Zarf, C., Lumsdon, A.E., Berlekamp, J., Tydecks, L., Tockner, K., 2015. A global boom in hydropower dam construction. *Aquat. Sci.* 77 (1), 161–170.
- Zhang, B., AghaKouchak, A., Yang, Y., Wei, J., Wang, G., 2019. A water-energy balance approach for multi-category drought assessment across globally diverse hydrological basins. *Agric. For. Meteorol.* 264, 247–265.
- Zhang, H., Gorelick, S.M., Zimba, P.V., Zhang, X., 2017. A remote sensing method for estimating regional reservoir area and evaporative loss. *J. Hydrol.* 555, 213–227. <https://doi.org/10.1016/j.jhydrol.2017.10.007>.
- Zhao, G., Gao, H., 2018. Automatic correction of contaminated images for assessment of reservoir surface area dynamics. *Geophys. Res. Lett.* 45 (12), 6092–6099. <https://doi.org/10.1029/2018GL078343>.

Zhao, G., Gao, H., 2019a. Estimating reservoir evaporation losses for the United States: Fusing remote sensing and modeling approaches. *Remote Sens. Environ.* 226, 109–124. <https://doi.org/10.1016/j.rse.2019.03.015>.

Zhao, G., Gao, H., 2019b. Towards global hydrological drought monitoring using remotely sensed reservoir surface area. *Geophys. Res. Lett.* 46 (22), 13027–13035.

Zhan, S., Song, C., Wang, J., Sheng, Y., Quan, J., 2019. A global assessment of terrestrial evapotranspiration increase due to surface water area change. *Earth's Future* 7 (3), 266–282.